32nd URSI GASS, Montreal, 19–26 August 2017

The Effect of Rounding the Corners of Scattering Structures: E-polarisation case

Paul D. Smith*(1) and Audrey J. Markowskei(1)
(1) Macquarie University, Sydney 2109, Australia, http://www.mq.edu.au

Abstract

In studying electromagnetic wave diffraction from scatterers with corners, a common approach is to first round the corners, thus producing a smooth surface, and eliminating the singularities introduced by the corners. Numerical methods based upon integral equation formulations can then be readily applied. In order to quantify the effect of such corner rounding we examine the two-dimensional case of diffraction from cylindrical scatterers which possess corners, that is, points at which the normal changes discontinuously. We employ a numerical method for the scattering of a E-polarised plane wave normally incident on a perfectly conducting cylindrical structures of constant cross-section and which may include corners. We assess the impact on near- and far-field scattering, as a function of the radius of curvature in the vicinity of the rounded corner point. We conclude by quantifying the rate of convergence of the maximum difference between the far-field solutions as that radius of curvature of the rounded scatterer approaches zero.

1 Introduction

Diffraction of electromagnetic waves by canonical shapes and structures of more general and arbitrary shape is of enduring interest. The choice of an appropriate canonical structure to model the dominant features of a scattering scenario can be very illuminating. Scattering by sharp edges and corners is informed by, for example, the diffraction from the half-plane and the wedge (of infinite extent). The nature of the singularities in the field and its derivatives is described in [1]. When numerical methods are employed, a common approach for dealing with domains with corners is to round the corners, producing a smooth surface. This eliminates the singularities introduced by the corners and enables the use of integral equation methods which are advantageous in the low frequency and resonance regimes [2].

Although there is an extensive literature on diffraction from sharp cornered objects as well as those with smooth boundaries, there does not seem to be a systematic treatment of the transition from one to the other, in particular as the radius of curvature of the rounded corner points tends to zero.

In order to clarify and quantify these effects this paper examines the diffraction from perfectly electrically conducting (PEC) cylindrical scatterers which possess corners, that is, points at which the normal changes discontinuously. We use a suitable numerical method for E-polarized electromagnetic plane waves incident on cylindrical structures possessing some points of small or zero curvature (that is, having a sharp corner). Earlier work in [3], [4] and [5] is significantly extended. The boundary condition is enforced at all points on the cross-sectional boundary of the cylinder. We implement the Nyström method expounded by [2] and adapt it for multi-cornered scatterers. These numerical methods are first used to compare the convergence of solutions for different discretizations of the surfaces of the scatterers, and then to assess the impact on near- and far-field scattering, as a function of the radius of curvature in the vicinity of the rounded corner point, of observation angle and as the frequency of the plane wave increases. We conclude by quantifying the rate of convergence of the maximum difference between the far-field solutions as the radius of curvature near the rounded corners approaches zero.

2 Problem Formulation

Consider an infinitely long cylinder with uniform cross section, and axis parallel to the z-axis. The cylinder is illuminated by an incident plane wave propagating with direction parallel to the x-y plane. The cross-section D lying in the x-y plane has a closed boundary ∂D parameterised by

$$x(t) = (x_1(t), x_2(t)), \qquad t \in [0, 2\pi]\,. \tag{1}$$

In this work, we consider three scatterers with one, two or four corners, respectively, and the scatterers that result after the corners have been rounded. The single-cornered lemniscate has parametrisation

$$x = x(t) = a\,(2\sin(t/2), -\sin t)\,, \qquad t \in [0, 2\pi], \tag{2}$$

where a is a parameter, henceforth set equal to 1 length unit. It has the corner at $t = 0$. The families of curves with rounded corners are parameterised by the quantity $\varepsilon\,(0 \le \varepsilon \le 1)$. The rounded lemniscate has representation

$$x = x(t) = a\left(2\sqrt{\varepsilon^2 + (1-\varepsilon^2)\sin^2(t/2)}, -\sin t\right), \tag{3}$$

where $t \in [0, 2\pi]$. The two-cornered scattered scatterer described by the parametric representation

$$x = x(t) = a\,(\cos t, \sin t)\,/\,(1 + |\sin t|)\,, \qquad t \in [0, 2\pi], \tag{4}$$

where a is again a unit length unit, has corners at $t=0$ and $t=\pi$. The rounded form is

$$x = x(t) = a\left(\frac{\cos t}{1+\sqrt{\varepsilon^2+\sin^2 t}}, \frac{\sin t}{1+\sqrt{\varepsilon^2+\sin^2 t}}\right). \quad (5)$$

The four-cornered scatterer has parametric representation

$$x = x(t) = \left(a(\cos t - \sin t), b(\cos t + \sin t)\right)/\hat{R}, \quad (6)$$

where $\hat{R}$=$(|\cos t| + |\sin t|)$, so that corners occur at $t=0$, $\pi/2$, π and $3\pi/2$ respectively; the parameters a and b are set to unit length unit, so that the resultant shape is a square. The corners are rounded using the representation

$$x(t) = (\cos t, \sin t)/R, \quad (7)$$

where R=$\left(\left(\frac{\cos t}{a}\right)^{1/\varepsilon} + \left(\frac{\sin t}{b}\right)^{1/\varepsilon}\right)^{\varepsilon}$. The corners of the all scatterers have an interior right angle, and the radius of curvature ρ at the rounded corner points is readily calculated.

The incident field illuminating the scatterer induces a scattered field; both are assumed time harmonic with a temporal factor $e^{-i\omega t}$. The spatial component $u^{\text{inc}}(x,y)$ of the incident wave travelling in the direction of the unit vector d=$(\cos\theta_0, \sin\theta_0)$ takes the form $u^{\text{inc}}(x,y) = e^{ikx\cdot d}$ where k is the wavenumber in the medium or in free space.

The spatial component $u^{\text{sc}}(x,y)$ of the scattered field obeys the Helmholtz equation at all points (x,y) exterior to the body; moreover it obeys the two-dimensional form of the Sommerfeld radiation condition as well as the finiteness of energy condition in the vicinity of the corners. Finally, the PEC scatterer requires the total field $u^{\text{tot}} = u^{\text{inc}} + u^{\text{sc}}$ at the boundary of the scatterer ∂D satisfy the Dirichlet condition $u^{\text{tot}}(x) = 0$ where $x \in \partial D$.

3 Integral Representations

We define two operators associated with the single- and double-layer potentials of a continuous density $\phi(y)$ defined on the boundary ∂D,

$$(\mathscr{S}\phi)(x) = 2\int_{\partial D} G(x,y)\phi(y)ds(y), \quad (8)$$

$$(\mathscr{K}\phi)(x) = 2\int_{\partial D} \frac{\partial G(x,y)}{\partial n(y)}\phi(y)ds(y) \quad (9)$$

where G is the 2-D free-space Green's function

$$G(x,y) = \frac{i}{4}H_0^{(1)}(k|x-y|), \quad (10)$$

and $H_0^{(1)}$ is the Hankel function of first kind and order zero.

The solution to the exterior Dirichlet problem is given by

$$u^{\text{sc}}(x) = \int_{\partial D}\left\{\frac{\partial G(x,y)}{\partial n(y)} - i\eta G(x,y)\right\}\phi(y)ds(y),\ x \in R^2\backslash\bar{D}, \quad (11)$$

where η is a coupling parameter, provided the continuous density $\phi(x)$ is a solution to the integral equation on ∂D:

$$\phi + \mathscr{K}\phi - i\eta\mathscr{S}\phi = -2g, \quad (12)$$

where $g = u^{\text{inc}}$. Uniqueness and solubility conditions for the problem are discussed in [2].

4 Numerical Solution

We use the Nyström method outlined in [2] to approximate the solution to the integral equation (11). Using the boundary parametrisation (1), the operator $\mathscr{S}\phi$ (8) becomes

$$(\mathscr{S}\phi)(x(t)) = \int_0^{2\pi} S_0(t,\tau)\phi(\tau)d\tau, \quad (13)$$

where $\phi(\tau)$=$\phi(x(\tau))((x_1'(\tau))^2 + (x_2'(\tau))^2)^{1/2}$ for some kernel $S_0(t,\tau)$. Similarly, the operator $\mathscr{K}\phi$ (9) generates an associated kernel $K_0(t,\tau)$. Thus we transform the formulation (12) to the integral equation for $0 \le t \le 2\pi$:

$$\phi(t) + \int_0^{2\pi}\{K_0(t,\tau) - i\eta S_0(t,\tau)\}\phi(\tau)d\tau = -2g(t). \quad (14)$$

The quadrature rules developed by Martensen and Kussmaul [2] to treat the logarithmic singularities arising in (8) and (9) employed: the singular parts of the kernels $S_0(t,\tau)$ and $K_0(t,\tau)$ are isolated in the for

$$\hat{K}_0(t,\tau) = \hat{K}_1(t,\tau)\ln\left(4\sin^2\frac{t-\tau}{2}\right) + \hat{K}_2(t,\tau), \quad (15)$$

where $\hat{K}_1, \hat{K}_2$ are analytic. The smooth components of the kernels are approximated using the trapezoidal rule; the logarithmically singular kernels are approximated using a weighted trigonometric interpolation quadrature. The resulting system of $2n$ linear equations thus discretizes (12).

Various spacings of a mesh of $2n$ points were used. For smooth scatterers we began by using uniformly spaced points $t_j = \pi j/n$, for $j = 0, 1, \ldots, 2n-1$, in the parameterisation (1). However, for domains with corners, the solution to (12) has singularities in the derivatives in the corners and to deal effectively with them, the uniform mesh is replaced by a non-uniform graded mesh [2]. An appropriate variable substitution $t = w(s)$ is performed so that the derivatives of the transformed integrand vanish up to a certain order at the corners and that approximately half of the quadrature points are uniformly distributed around the surface of the scatterer between the corners with the other half are concentrated at the corners. Thus the definite integral over $[0, 2\pi]$ of any function $f(t)$ is evaluated by trapezoidal quadrature after the substitution:

$$\int_0^{2\pi} f(t)\,dt = \int_0^{2\pi} f(w(s))\,w'(s)\,ds \approx \frac{\pi}{n}\sum_{j=1}^{2n-1} a_j f(s_j), \quad (16)$$

with weights $a_j = w'(t_j)$ and mesh points $s_j = w(t_j)$.

For domains with corners, the corners are assumed to be located at the points x_i on the scatterer boundary ∂D, and $\partial D \backslash \bigcup \{x_i\}$ is assumed to be C^2 and piecewise analytic. The angle γ_i at the corners is assumed to lie in the interval $0 < \gamma_i < 2\pi$. The function $w(s)$ must be strictly monotonically increasing between the corners and the derivatives at the corners must vanish up to some order p. For a domain with a single corner, we used the function $w(s)$ recommended by [2], and for the scatterers with two or four corners our choice of function $w(s)$ is discussed in [5]. The appropriate substitution is applied to the kernels S_0 and K_0 and is then discretized as before. Each of the above four quadrature rules evaluated at the $2n$ points t_j produce a system of $2n$ linear equations which are solved the usual Gaussian elimination procedure.

Although implementation of the graded mesh ensures a rapid convergence rate (as a function of n) for scatterers with corners and the Neumann and impedance boundary conditions [5], a further modification for the Dirichlet boundary condition is necessary to achieve comparable convergence rates. For these domains the kernel of (11) is no longer weakly singular at the corner. For domains with a single corner at x_0 we follow the technique of [2] using the fundamental solution

$$G_0(x,y) = \frac{1}{2\pi} \ln \frac{1}{|x-y|}, \qquad x \neq y, \tag{17}$$

of the Laplace equation in R^2 to subtract a vanishing term. This transforms (11) into

$$u^{\mathrm{sc}}(x) = \int_{\partial D} \left\{ \frac{\partial G(x,y)}{\partial n(y)} - i\eta G(x,y) \right\} \phi(y), \\ - \frac{\partial G_0(x,y)}{\partial n(y)} \phi(x_0) ds(y); \qquad x \in R^2 \backslash \bar{D}, \tag{18}$$

the associated boundary equation (12) is reformulated as

$$\phi(x) - \phi(x_0) + 2 \int_{\partial D} \left\{ \frac{\partial G(x,y)}{\partial n(y)} - i\eta G(x,y) \right\} \phi(y) ds(y) \\ - 2 \int_{\partial D} \frac{\partial G_0(x,y)}{\partial n(y)} \phi(x_0) ds(y) = -2u^{\mathrm{inc}}(x), \; x \in \partial D. \tag{19}$$

An analysis showing the existence of a solution to (19) is provided in [2]. This modification needs to be extended when the scatterer has more than one corner on ∂D. The details are in [5]. In all cases we apply the substitution (16) with graded mesh, discretize and solve as previously described. The described modifications applied to (11) and (12) ensure that rapid convergence is achieved for scatterers with corners and the Dirichlet boundary condition on ∂D.

A detailed set of numerical experiments on the scatterers defined above and their rounded counterparts in described in [5]. It is shown that a graded mesh is essential to achieve a convergent solution for each of the sharp-cornered objects; moreover it is vastly more efficient to use a graded mesh approach for the rounded counterparts, and as the radius of curvature at the rounded corner becomes small, a graded mesh becomes essential to achieve convergence.

5 The Effect of Rounding on Scattered Field

We now measure the deviation from the solution produced by a cornered scatterer to that produced when the corners are rounded. For all experiments the appropriate graded mesh was used on both the cornered scatterers and those where the corners were rounded. The far-field is

$$u^{\infty}(\hat{x}) = \frac{e^{-i\frac{\pi}{4}}}{\sqrt{8\pi k}} \int_{\partial D} \{ kn(y) \cdot \hat{x} + \eta \} e^{-ik\hat{x}\cdot y} \phi(y) ds(y), \tag{20}$$

in the direction $\hat{x}$ ($|\hat{x}| = 1$). The difference between the solution $u_0^{\infty}(\hat{x})$ produced by a cornered scatterer, and that produced by rounding, $u_\rho^{\infty}(\hat{x})$, with associated radius of curvature ρ, is measured by

$$\left\| u_0^{\infty} - u_\rho^{\infty} \right\|_2 = \left(\int_0^{2\pi} \left| u_0^{\infty}(\hat{x}) - u_\rho^{\infty}(\hat{x}) \right|^2 d\hat{x} \right)^{\frac{1}{2}}, \tag{21}$$

$$\left\| u_0^{\infty} - u_\rho^{\infty} \right\|_\infty = \max_{\hat{x} \in [0,2\pi]} \left| u_0^{\infty}(\hat{x}) - u_\rho^{\infty}(\hat{x}) \right|. \tag{22}$$

These tests were run for all three scatterers with the Dirichlet boundary conditions for a range of values of ka ($1 \leq ka \leq 16\pi$) and radii of curvature ρ ($0.00125 \leq \rho \leq 0.1$). The differences decreased monotonically to zero as $k\rho$ goes to zero. Typical results with $ka = 2\pi$ and $\hat{x} = (1,0)$ obtained when comparing rounded structures to sharp-cornered ones with $\rho = 0.02$ are as follows. For the lemniscate, the differences in the L^2 norm and L^∞ norm are 2.4% and 1.4%, respectively. For the two corner and four corner scatterers, the L^2 norm differences are 3.2% and 1.3%, respectively. These differences increase as ρ increases. We also found that for a given ρ the two-cornered scatterer has higher percentage differences for the norms compared to those of the lemniscate or the square. This is attributable to two factors: the choice of function for the graded mesh and the smaller cross-sectional area of the two-cornered scatterer. In the case of the lemniscate and square, the derivatives vanish up to order $p = 8$, whereas for the two-cornered scatterer the choice of function has $p = 6$. Choosing a function with a higher-order p is expected to reduce this difference.

Interest also naturally focusses on those observation points at which the far-fields most noticeably differ. In all cases, the greatest differences in the far-fields of the rounded and unrounded scatterers occur in the back-scatter region. Physically this is attributable to the difference in the scattering mechanisms in the locality of the corner. Also as expected, as the radius of curvature decreases, the difference between the fields is minimised. Conversely, for given radius of curvature ρ, the differences increase as the wavenumber increases and are again most noticeable in the back-scatter

region. As ka increases, the wavelength of the illuminating field becomes smaller so that the amount of corner removed by rounding becomes more significant.

The far-field differences are dependent on the angle of the incident plane wave θ_0 relative to the corner. For example when the incident wave is travelling in the direction that first makes contact with the broad end of the lemniscate, the two fields are nearly identical, even with $\rho = 0.05$ and $ka = 2\pi$. The actual maximum difference between the fields (22) is 4×10^{-3}: a relative difference of 0.2%.

We examined the behaviour of the non-dimensionalised far-field difference $\sqrt{k}\left\|u_0^\infty - u_\rho^\infty\right\|_\infty$. Using a least square fit to the data (see Figure 1), for $k\rho \leq 0.25$, we found that

$$\sqrt{k}\left\|u_0^\infty - u_\rho^\infty\right\|_\infty \approx C(\theta_0)(k\rho)^m, \tag{23}$$

for some constant C dependent on the direction of the plane wave, θ_0, and some constant m; the results show that for the Dirichlet condition $m \approx 4/3$ (independent of θ_0).

6 Conclusion

Numerical methods based upon integral equations were employed to study the effect of rounding the corners of PEC scatterers. Graded meshes were essential in obtaining convergent results as the radius of curvature near rounded corners decreases. The differences in the far-fields of various scatterers and their rounded counterparts satisfy $\sqrt{k}\left\|u_0^\infty - u_\rho^\infty\right\|_\infty \approx C(\theta_0)(k\rho)^{4/3}$ as $k\rho \to 0$. Analytic studies to support this conclusion are in progress.

References

[1] Bowman, J., T. Senior, and P. Uslenghi (1987), *Electromagnetic and acoustic scattering by simple shapes (Revised edition)*, vol. 1, Hemisphere Publishing Corp., New York.

[2] Colton, D. L., and R. Kress (2013), *Inverse acoustic and electromagnetic scattering theory*, Applied mathematical sciences, 3rd ed., xiv, 405 p. pp., Springer, New York.

[3] Smith, P. D., A. Markowskei, and A. D. Rawlins (2014), Two-dimensional diffraction by impedance loaded structures with corners, in *Electromagnetics in Advanced Applications (ICEAA), 2014 International Conference on*, pp. 644–647.

[4] Smith, P. D., and A. J. Markowskei, The diffractive effect of rounding the corners of scattering structures, in *Electromagnetics in Advanced Applications (ICEAA), 2015 International Conference on*, pp. 1592–1595.

[5] Smith, P. D., and A. J. Markowskei, What effect does rounding the corners have on diffraction from structures with corners?, in *Advanced Electromagnetic Waves*, edited by S. Bashir, InTech.

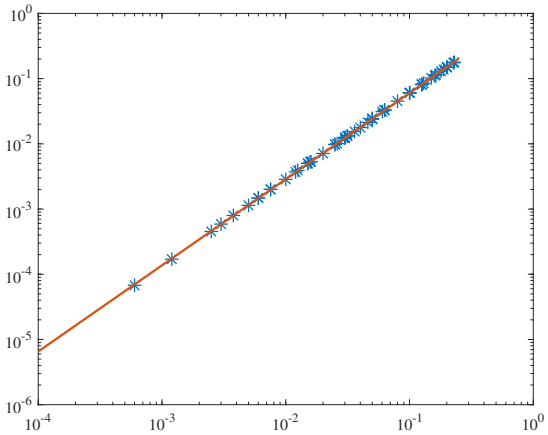

(a) Lemniscate, $\theta_0 = 0$

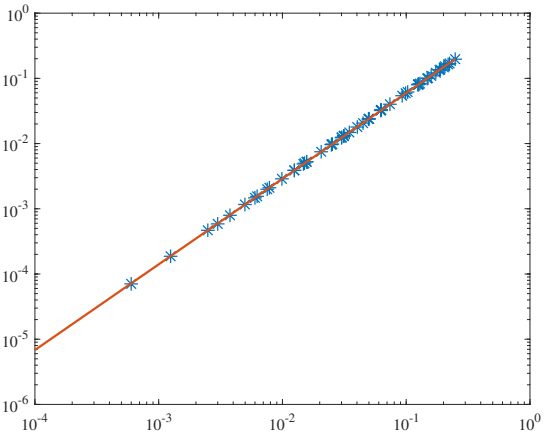

(b) Two-corner, $\theta_0 = 0$

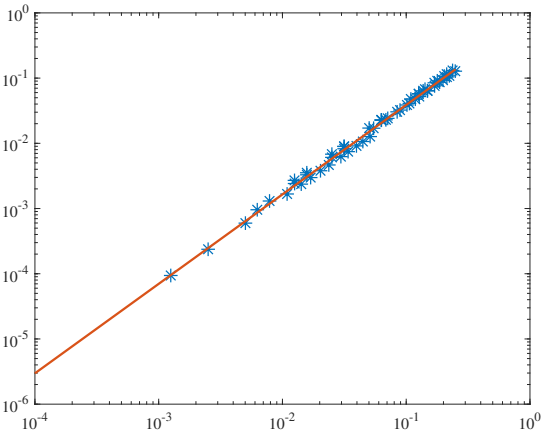

(c) Square, $\theta_0 = \pi/4$

Figure 1. Logarithmic plot: $x = k\rho$, $y = \sqrt{k}\left\|u_0^\infty - u_\rho^\infty\right\|_\infty$. Illustrating the least square fit. The data points used are represented by the blue asterisks, the least square line of fit is shown in red.